Cureus Journal of Engineering

Open Access Original Article

Simulation, Fabrication, and Characterization of Bismuth Oxide-Ethylene Vinyl Acetate (Bi2O3-EVA) Composite As a Cesium-137 Gamma Radiation Shield

Received 04/28/2025
Review began 05/12/2025
Review ended 08/15/2025
Published 09/01/2025

DOI:
https://doi.org/10.7759/s44388-025-05226-z

Kyle Noah D. Esguerra [1] , Jan Isiah S. Dela Cruz [1] , John Dominic L. Sapao [1] , Randy Joseph G. Fernandez [1]

1. Philippine Science High School - Central Luzon Campus, DOST-Philippine Science High School System, Mabalacat City, PHL

Corresponding author: Kyle Noah D. Esguerra, kekesgue@gmail.com

Abstract

Prolonged exposure to cesium-137 (Cs-137) gamma radiation, a high-energy source widely used in medicine, is known to cause cellular damage and increased rates of cancer. Wearable lead-lined radiation shields provide a direct protective barrier that attenuates ionizing radiation. Aside from being toxic, lead is heavy and rigid-this limits the dexterity of medical workers. Non-toxic polymer composites are promising solutions as they combine high attenuation rates of high-density materials with the lightness and flexibility of polymers. In this study, a composite consisting of bismuth oxide and ethylene vinyl acetate (Bi_2O_3-EVA) was simulated, fabricated, and characterized to determine its structural and radiation shielding performance. The simulation results determined that increasing Bi_2O_3 filler content enhances shielding performance. Bi_2O_3-EVA composites were then fabricated through melt-mixing methods and compression molding. Radiation shield testing showed that composites with higher Bi_2O_3 filler content displayed improved shielding efficiencies, with higher linear attenuation coefficients and lower half-value layer thicknesses. Samples consisting of 60% Bi_2O_3 by weight produced optimal shielding performance, achieving half-value layer values between 1.508 cm and 1.878 cm. Analysis of homogeneity levels through the ISO-based rapid comparative method and texture analysis yielded acceptable values, entailing that its consistent structure does not compromise radiation shielding performance. Moreover, the tensile strength is maintained even at a high 80% Bi_2O_3 by weight. The positive results obtained in this study present new opportunities for developing lighter and more flexible wearable medical gamma radiation shields that effectively attenuate gamma radiation.

Categories: Materials Engineering, Nuclear Energy, Polymer Science and Engineering
Keywords: cesium-137, bismuth oxide, ethylene vinyl acetate, gamma radiation, radiation shield

Introduction

Cesium-137 (Cs-137) is extensively used in medical fields such as radiotherapy, cancer brachytherapy, and blood irradiation [1]. Cs-137 emits gamma radiation, a high-energy source that can displace electrons from molecules [2]. Prolonged exposure to gamma radiation is associated with numerous health risks, such as higher rates of cancer, genetic damage, and cardiovascular problems [3-5]. Direct protective barriers, such as wearable radiation shields, reduce exposure to prevent harmful effects [6]. Viable shields are fabricated using materials with the following properties: homogeneous formulation, high density, high tensile strength, long lifetime degradation, high shielding efficiency, high linear attenuation coefficients (LAC), and low half-value layer (HVL) [7].

Conventional radiation shields use lead as a primary material due to its superior shielding properties and ease of production [8]. However, lead is highly toxic when ingested, causing approximately 1 million casualties per year [9]. Additionally, lead-lined equipment is heavy and rigid, limiting the dexterity and mobility of medical workers [10]. Medical workers would benefit from radiation shields of less harmful alternatives, such as metal-polymer composites. These non-toxic composites combine the lightness and flexibility of polymers with the high densities of metal additives [11,12]. For example, a 2 mm sheet of tungsten carbide-ethylene vinyl acetate (WC-EVA) has a shielding efficiency of 93 ± 0.2%, higher than lead of the same thickness with a shielding efficiency of 80%; it also exhibits enhanced flexibility and elasticity brought about by the EVA [13]. On the other hand, using WC is more expensive than fabricating lead [8]. Therefore, other cost-efficient metal fillers should be investigated with polymer composites.

An emerging replacement for WC is bismuth oxide (Bi_2O_3) [14]. When combined with polymer composites, Bi_2O_3 can provide effective shielding performance at a lighter weight and cheaper cost than WC [15]. Bi_2O_3 has been tested with several polymers, such as polyvinyl chloride (PVC), producing one of the highest shielding efficiencies of polymer-metal composites [16]. On the other hand, EVA shows better resistance and flexibility under radiation damage than PVC [17]. However, limited studies have tested this compound alongside EVA. Pursuing EVA alongside Bi_2O_3 holds immense potential in providing high shielding performance while being light and flexible.

This study evaluated the performance of the Bi_2O_3-EVA composite as a Cs-137 gamma radiation shield. The study simulated the shielding performance in terms of LAC and HVL. In addition, composites of different weight ratios were fabricated. Finally, the fabricated samples were characterized in terms of homogeneity, tensile strength, shielding efficiency, LAC, and HVL. The results of this study are a potential stepping stone in improving medical radiation protection by producing alternative shields that can effectively protect medical workers while reducing weight and increasing flexibility. Furthermore, manufacturers of radiation shields can benefit from lower costs and easily produced materials, thereby increasing the accessibility of wearable radiation shields.

Materials And Methods

The study had four main stages: analytical methods, sample fabrication, experimental measurements, and interpretation of results. Analytical methods consisted of the simulation of shielding properties through software. Sample fabrication was done through melt-mixing and molding. Experimental measurements included testing on structural and shielding properties. Finally, results were interpreted through statistical analysis.

Varying weight ratios of Bi_2O_3 in the Bi_2O_3-EVA composite were used, from 0% to 80% in increments of 10%, as shown in Table *1*.

Code	Bi_2O_3 (wt %)	EVA (wt %)
B-0	**0**	**100**
B-10	10	90
B-20	20	80
B-30	30	70
B-40	40	60
B-50	50	50
B-60	60	40
B-70	70	30
B-80	80	20

TABLE 1: Simulation design for radiation shield Bi2O3-EVA composites

Bi2O3-EVA, bismuth oxide-ethylene vinyl acetate

The composite density was computed from the density of Bi_2O_3 ($\rho_{\mathrm{Bi_2O_3}}$), % weight of Bi_2O_3 ($w_{\mathrm{Bi_2O_3}}$), density of EVA (ρ_{EVA}), and % weight of EVA (w_{EVA}) [18]:

$$\rho_{\mathrm{composite}} = \frac{100}{\frac{w_{\mathrm{Bi_2O_3}}}{\rho_{\mathrm{Bi_2O_3}}} + \frac{w_{\mathrm{EVA}}}{\rho_{\mathrm{EVA}}}}$$

Additionally, the percent heaviness compared with lead were computed from the composite density ($\rho_{\mathrm{composite}}$) and the density of lead (ρ_{Pb}) [19]:

$$\%\mathrm{heaviness} = \frac{\rho_{\mathrm{composite}}}{\rho_{\mathrm{Pb}}} * 100$$

Afterward, LAC and HVL were simulated using EpiXS 2.0.1 Dark [20] and Phy-X/PSD [21]. Values for all weight ratios were extracted for Cs-137 at 661.657 keV.

Table 2 shows different weight ratios of the fabricated composites consisting of Bi_2O_3 filler dispersed in the EVA matrix. Bi_2O_3 powder (CAS Number 1304-76-3) was procured at an online marketplace, while the EVA pellets (HANWHA EVA 1326) were obtained from the stock of a local shoe factory.

Code	Bi_2O_3 (wt %)	EVA (wt %)
B-0	0	100
B-40	40	60
B-50	50	50
B-60	60	40
B-70	70	30
B-80	80	20

TABLE 2: Experimental design for radiation shield Bi2O3-EVA composites

The ratios of composites were adapted from Soylu et al. [13]. Bi2O3-EVA, bismuth oxide-ethylene vinyl acetate

The pellets and powder were melted and mixed at approximately 130℃ using a two-roll mill in the Materials Science Division of the Department of Science and Technology - Industrial Technology Development Institute (DOST-ITDI). The two-roll mill serves to “disperse and distribute the compound additives in a manner that will affect the physical properties of the compound” [22]. Afterward, the melted ingredients were poured into an 8" × 8" steel square mold and placed on a compression molding machine for 5 minutes until a sheet was produced with a thickness of 0.2 cm. The fabricated composites were placed in sealed plastic bags before and after testing, to prevent contamination. Additionally, these composites were stored at normal room temperature. Samples of fabricated composites are shown in Figure 1.

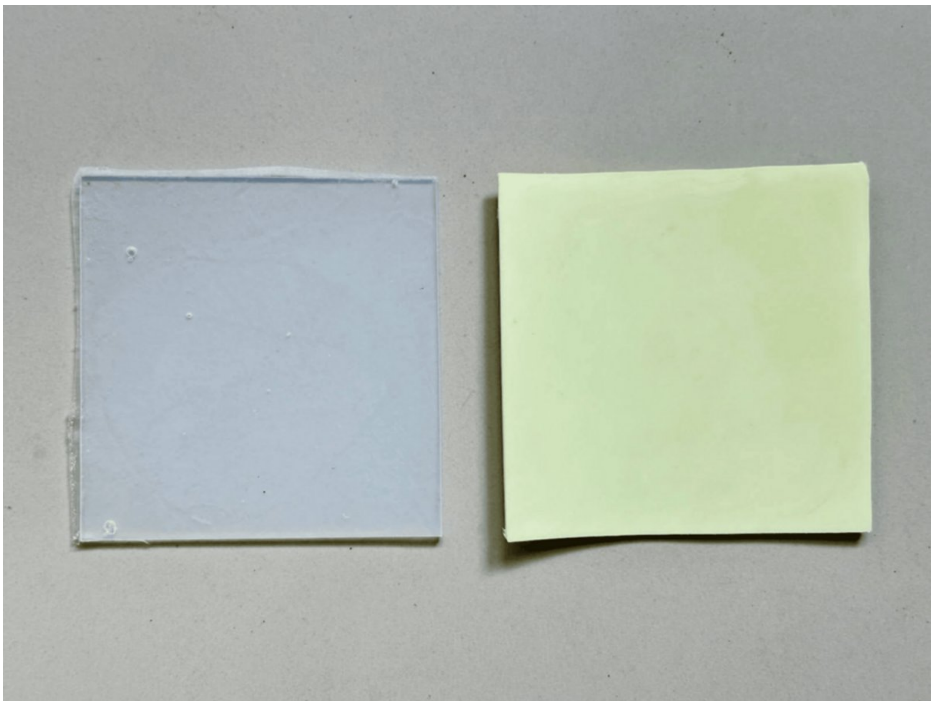

FIGURE 1: Fabricated Bi2O3-EVA composite samples

Fabricated samples of pure EVA (left) and 60% Bi_2O_3 by weight (right). Bi2O3-EVA, bismuth oxide-ethylene vinyl acetate

High-resolution magnified (300×) images of the samples were obtained using a scanning electron microscope (SEM) in the Philippine Science High School - Ilocos Region Campus (PSHS-IRC). Images were scanned in three regions (upper right, middle, and lower left) of each weight ratio. Qualitative evaluation was done using the rapid comparative method [23], a side-by-side visual analysis against photographic standards for carbon black and rubber mixtures. Like carbon black [24], similarly-sized bismuth oxide nanoparticles tend to agglomerate when added to polymer composites [25]. These similar properties illustrate the effectiveness of the rapid comparative method in evaluating the dispersion of particles with comparable sizes in equally flexible materials. Texture analysis was used to gauge homogeneity quantitatively by obtaining angular second moment (ASM) and inverse difference moment (IDM) values in ImageJ, an image processing software. Tensile strength was evaluated using a universal testing machine by determining the maximum force applied to the samples before breaking. Radiation shielding efficiency tests were conducted using a Cs-137 gamma source set 1 meter from the sample as prescribed by radiation testing standards from the Philippine National Research Institute and a Rotem Ram R-200 Survey Meter for the readings of the shielded and unshielded dose rates [26]. The configuration of the testing apparatus can be seen in Figure *2*.

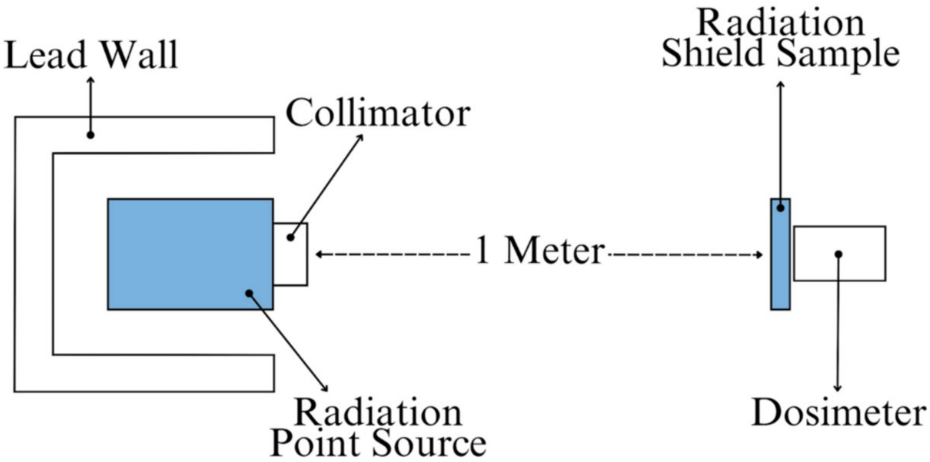

FIGURE 2: Radiation testing apparatus layout

The diagram shows a top view of the configuration of the radiation testing apparatus used in the Department of Science and Technology - Philippine Nuclear Research Institute.

Composite samples were subjected to gamma radiation from a Cs-137 source at 662 keV. To obtain the reference radiation dose (i.e., no shield applied), the dosimeter was placed in front of the radiation source for 10 seconds. Three dose values were obtained every 5 seconds.

The same process was done to obtain radiation dose values for varying concentrations of bismuth oxide filler content. Since there were two samples fabricated for each composite, a total of six data points were measured for every composite (B-0, B-40, B-50, B-60, B-70, and B-80).

The shielding efficiency of each sample was calculated from the shielded dose rate (D) and unshielded dose rate (D_o):

$$\mathrm{SE} = (1 - \frac{D}{D_o}) * 100$$

Additionally, the LAC was calculated from the shielding efficiency (SE) and thickness of the material (x) [7]:

$$\mu = \frac{ln(1 - \frac{\mathrm{SE}}{100})}{-x}$$

Finally, the half-value layer (HVL) was computed from the LAC (μ) [7]:

$$\mathrm{HVL} = \frac{ln(2)}{\mu}$$

Results

Structural evaluation

Following the computation of density and percent heaviness, trendlines were produced to observe their behavior as filler content increases. Moreover, homogeneity was qualitatively and quantitatively assessed using standardized procedures, while tensile strength is exhibited in a stress-strain diagram.

An increasing nonlinear association between the composition of the material (Bi_2O_3 filler in EVA matrix) and its computed density was observed. A Pearson's correlation indicated a very strong, positive, significant relationship, r(7) = .938, p < .001. A fourth-order polynomial approximation obtained the equation: $0.000947x^4 - 0.00884x^3 + 0.0411x^2 + 0.048x + 0.952$ with R^2 = 1.00.

An increasing nonlinear association between the composition of material (Bi_2O_3 filler in EVA matrix) and its computed percent heaviness using lead as standard was observed. A Pearson's correlation indicated a very strong, positive, significant relationship, r(7) = 0.938, p < .001. A fourth-order polynomial approximation obtained the equation: $0.00835x^4 - 0.0779x^3 + 0.362x^2 + 0.424x + 8.4$ with R^2 = 1.00.

The SEM micrographs of B-40 and B-80, taken at 300× magnification, exhibited visible cylindrical rod-like filler particles and streak-like patterns or striations highlighted in Figure 3. Qualitative analysis through the ISO-based rapid comparative method yielded two ratings for all samples. B-40, B-50, B-60, and B-70 all yielded a rating of 7, while B-80 was the sole sample that yielded a rating of 8, showing better homogeneity distribution than previous samples.

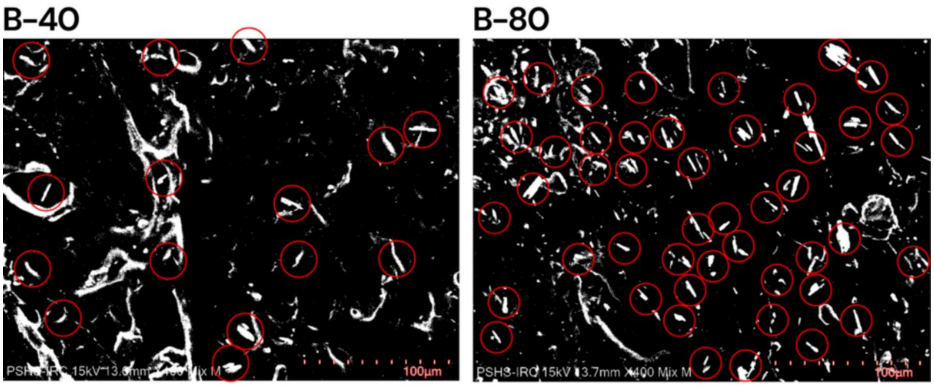

FIGURE 3: Rapid comparative evaluation of the homogeneity of B-40 and B-80 samples

SEM micrographs, at 300× magnification, of 40% Bi_2O_3 by weight (B-40, left) and 80% Bi_2O_3 by weight (B-80, right) were compared with photographic standards of ISO 11345:2006 [20]. The encircled shapes on the micrograph highlight Bi_2O_3 particles. SEM, scanning electron microscope

For the quantitative analysis, Figure 4 exhibits the box plot of the ASM values of the samples per weight ratio. The Kruskal-Wallis H test indicated that there are significant differences in the ASM values of varying weight ratios, $\chi^2(4)$ = 23.47, p < .001, with a mean rank score of 21.67 for B-40, 25.83 for B-50, 14.58 for B-60, 11.83 for B-70, 3.58 for B-80. Post-hoc comparisons through the Dunn's Test with a Bonferroni corrected alpha value of 0.0005 revealed that there were statistically significant differences in values between B-40 and B-80 (z = 3.5702, p < .001), and B-50 and B-80 (z = 4.3928, p < .001).

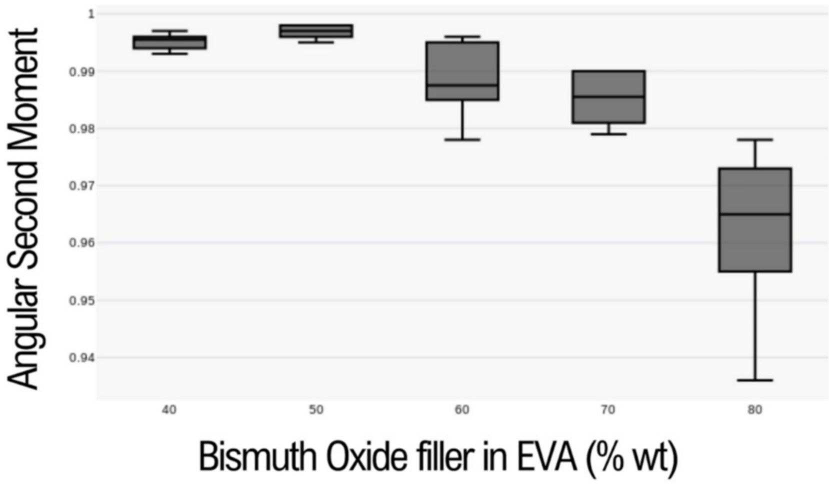

FIGURE 4: Angular second moments from varying Bi2O3 filler weight ratios

Each weight ratio consisted of two samples with SEM images taken in three regions (upper right, middle, and lower left) for homogeneity measurement. Bi2O3, bismuth oxide; EVA, ethylene vinyl acetate; SEM, scanning electron microscope

Figure 5 depicts the boxplot of the IDM values of the samples per weight ratio. The Kruskal-Wallis H test indicates that there are significant differences in the IDM values between varying weight ratios, $\chi^2(4) = 23.98$, $p < .001$, with a mean rank score of 21.75 for B-40, 25.5 for B-50, 14.42 for B-60, 12.33 for B-70, and 3.5 for B-80. Post-hoc comparisons using Dunn's Test with a Bonferroni corrected alpha value of 0.0005 revealed that there were statistically significant differences in values between B-40 and B-80 ($z = 3.684$, $p < .001$) and between B-50 and B-80 ($z = 4.441$, $p < .001$).

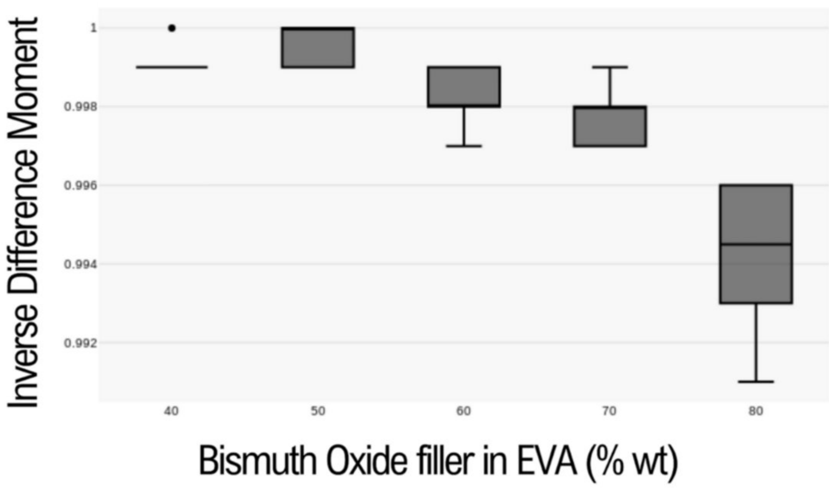

FIGURE 5: Inverse difference moments from varying Bi2O3 filler weight ratios

Each weight ratio consisted of two samples with three regions (upper right, middle, and lower left) for homogeneity measurement. Bi2O3, bismuth oxide; EVA, ethylene vinyl acetate

Figure 6 presents the association between the composition of material (Bi_2O_3 filler in EVA matrix) and its tensile strength. Results of the Pearson correlation indicated a very weak, positive, nonsignificant relationship, r(4) = .0802, p = .880.

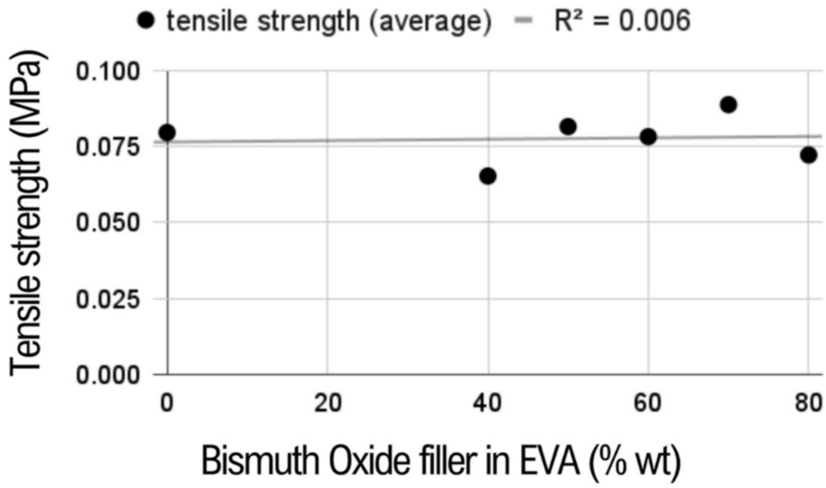

FIGURE 6: Tensile strengths of varying Bi2O3 filler weight ratios

Each weight ratio consisted of two samples for tensile strength measurement. Bi2O3, bismuth oxide; EVA, ethylene vinyl acetate

Shielding performance evaluation

Box plots were produced to display the association between the composition of the material and its shielding efficiency, linear attenuation coefficient, and half-value layer. Additionally, a comparison of simulation and experimental results was examined through trendline behavior.

Figure 7 shows a box plot of the shielding efficiency values for varying compositions of the material (Bi_2O_3 filler in EVA matrix). The Kruskal-Wallis H test indicated that there is a significant difference in the shielding efficiency values between the different compositions of the material, $\chi^2(5) = 18.24$, p = .003, with a mean rank score of 11.5 for B-0, 9.5 for B-40, 17.33 for B-50, 31.33 for B-60, 16.83 for B-70, and 24.5 for B-80. Post-hoc comparisons were conducted using Dunn's test with a Bonferroni corrected alpha of 0.0033. The difference between B-0 and B-60 clusters was statistically significant (z = 3.2735, p = .001). Additionally, the difference between the B-40 and B-60 clusters was statistically significant (z = 3.6036, p < .001). B-60 exhibits a superior shielding performance of 7.27% compared to the other weight ratios tested. The equivalent linear attenuation coefficient is 0.38 cm^{-1} and the half-value layer is 1.67 cm.

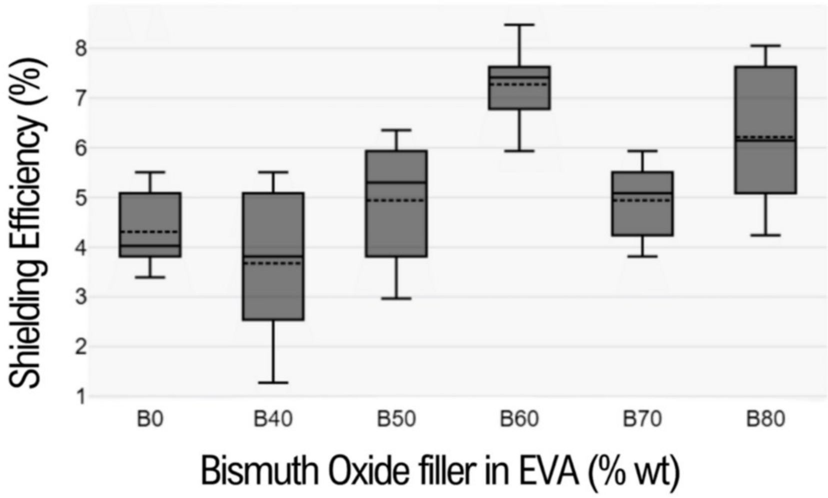

FIGURE 7: Shielding efficiencies of varying Bi2O3 filler weight ratios

Shielding efficiency values (n = 6) were obtained with the dosimeter placed at a 1-meter distance. Bi2O3, bismuth oxide; EVA, ethylene vinyl acetate

Table 3 presents the differences in simulated values, both for LAC and HVL, on EpiXS and Phy-X/PSD. The differences were computed from the simulations of both tools, with EpiXS as the reference. The percent differences for LAC range from 0.03% to 0.56%, while those of HVL span from 0.09% to 0.24%.

Code	Bi_2O_3 content (% wt)	Percent difference (%)	
		LAC	HVL
B-0	0	0.56	0.09
B-10	10	0.06	0.12
B-20	20	0.40	0.14
B-30	30	0.56	0.16
B-40	40	0.40	0.19
B-50	50	0.03	0.20
B-60	60	0.04	0.23
B-70	70	0.25	0.22
B-80	80	0.33	0.24
Lead	-	0.30	0.21

TABLE 3: Percent differences in simulated values between EpiXS and Phy-X/PSD

LAC, linear attenuation coefficients; HVL, half-value layer

Figure 8 presents a nonlinear association between the composition of material (Bi_2O_3 filler in EVA matrix) and the composite's LAC. A Pearson's correlation revealed a very strong, significant positive correlation for simulation results (r(4) = .918, p = .010) and a strong but nonsignificant correlation for experimental results (r(4) = .657, p = .157). A third-order polynomial approximation obtained equations of $0.00705x^3 - 0.00383x^2 + 0.0185x + 0.0774$ (R^2 = 0.615) for experimental and $0.000000968x^3 - 0.0000713x^2 + 0.00282x + 0.0795$ (R^2 = 1.00) for simulation.

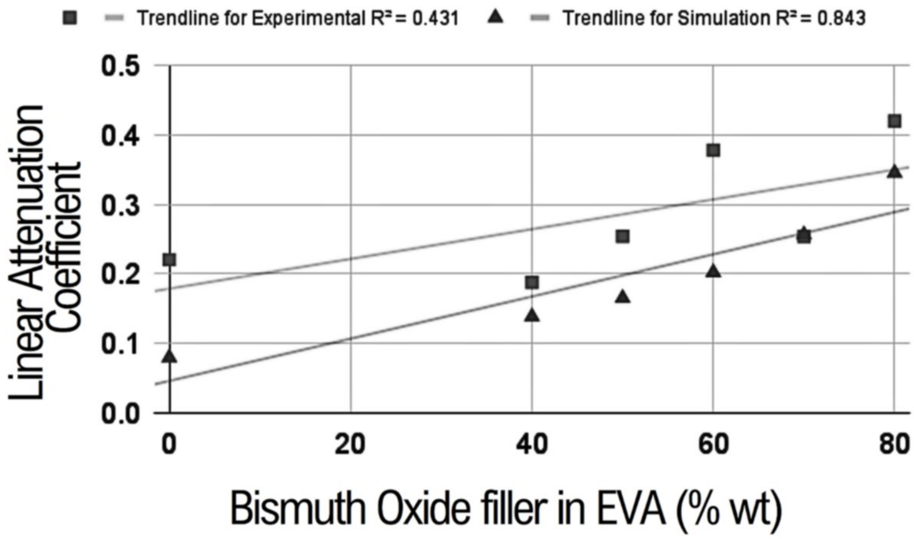

FIGURE 8: Simulated and experimental values of linear attenuation coefficients in varying Bi2O3 filler weight ratios

Simulation values were obtained from the averaged results from EpiXS and Phy-X/PSD. Bi2O3, bismuth oxide; EVA, ethylene vinyl acetate

Figure 9 presents a nonlinear association between the composition of material (Bi_2O_3 filler in EVA matrix) and its HVL. Results of the Pearson correlation indicated a strong, negative, nonsignificant relationship, r(4) = .633, p = .178 for experimental and a very strong, positive, significant relationship, r(4) = .998, p < .001 for simulation. A third-order polynomial approximation obtained equations of $0.00000858x^3 - 0.0013x^2 + 0.0419x + 2.23$ (R^2 = 0.665) for experimental results and $-0.000000551x^3 + 0.000288x^2 - 0.103x + 8.71$ (R^2 = 1.00) for simulation results.

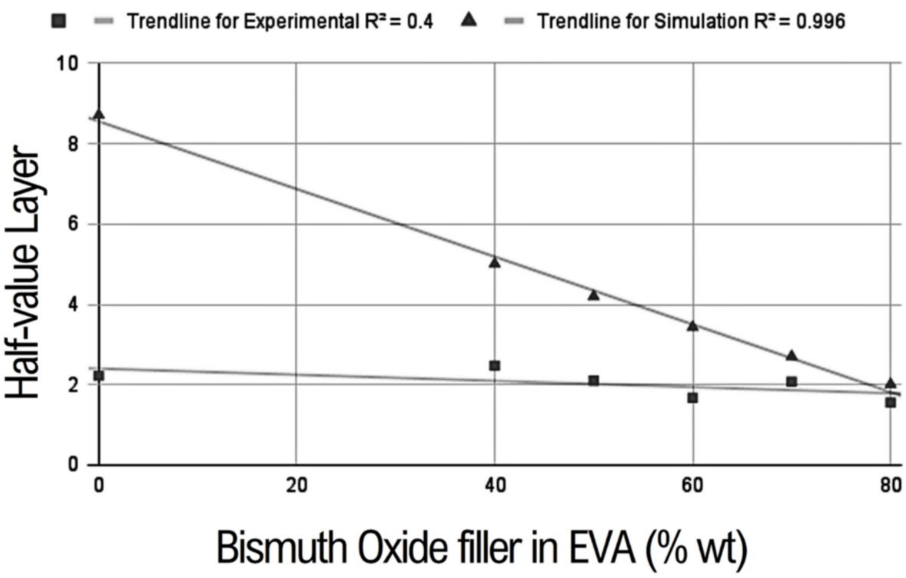

FIGURE 9: Simulated and experimental values of half-value layer in varying Bi2O3 filler weight ratios

Simulation values were obtained from the averaged results from EpiXS and Phy-X/PSD. Experimental values (n = 6) were obtained with a distance of 1 meter from the dosimeter. Bi2O3, bismuth oxide; EVA, ethylene vinyl acetate

Discussion

The incremental increase of bismuth oxide content by weight showed varying effects on the structural properties of the composite. The increase in the density and percent heaviness of the composite, along with the amount of Bi_2O_3 filler content, can be attributed to the filler's inherent heavy metallic properties that replace a portion of the lower-density polymer, increasing the overall composite density and weight [11]. On the other hand, this may cause the sample to be heavier and more rigid. The results align with related literature on polymer composites [7,27-29].

The highlighted cylindrical and rod-like shapes and striations in Figure *6* match those in related literature on the appearance of Bi_2O_3 and EVA [30,31]. This confirms that the filler has successfully mixed with the matrix. Samples with a rating of 7 showed a uniform dispersion of filler particles despite farther distances between each other, while samples with a rating of 8 exhibited a higher amount of filler content, resulting in more compressed but still uniform particle distances.

Quantitative homogeneity analysis affirmed the sample's exhibited acceptable homogeneity levels. The statistically significant differences between B-40 and B-80, and B-50 and B-80 showed that ASM and IDM may drastically vary as the filler content augments. Furthermore, it can be observed that all SEM images produced ASM and IDM values near 1, which indicates a uniform and homogeneous particle dispersion [32-34].

Tensile strength analysis suggests that the addition of Bi_2O_3 may not have a significant effect on the tensile strength of the composite. The small changes in tensile strength values indicate that EVA predominantly influences the mechanical properties of the composite. This finding contrasts with related literature, which suggests that Bi_2O_3 may affect mechanical properties, often reporting that increasing the amount of Bi_2O_3 filler content reduces tensile strength [35,36].

The low percent differences between simulations of LAC and HVL from EpiXS 2.0.1 Dark and Phy-X/PSD exhibit a high degree of congruence despite using software tools that utilize different libraries. This close alignment suggests a strong level of agreement between the two simulation tools in evaluating the gamma radiation shielding performance across different weight ratios.

Shielding performance testing exhibits that increasing Bi_2O_3 filler content leads to improved shielding performance. Notably, samples consisting of 60% Bi_2O_3 by weight have the superior shielding performance among all tested weight ratios as measured by shielding efficiency. Moreover, higher Bi_2O_3 content is desirable for radiation shields since it reduces the thickness for the same amount of shielding efficiency. These findings align with related literature on polymer composites [37,38]. The mechanical properties of the composite may have been negatively affected at higher concentrations of filler, resulting in a reduction in matrix flexibility and increased brittleness [39].

Conclusions

The findings show opportunities in developing flexible and effective Cs-137 gamma radiation shields from a composite made of Bi_2O_3 and EVA. A homogeneous dispersion of Bi_2O_3 filler ensures consistent attenuation of gamma radiation along the surface of the composite. On the other hand, tensile strength testing shows that EVA predominantly influences the mechanical properties of the composite. Simulations show that increasing Bi_2O_3 filler content provides better shielding performance; meanwhile, experimental results indicate the superior performance of 60% Bi_2O_3 by weight among all tested weight ratios. This emphasizes the need to conduct more extensive tests when developing shielding materials.

Future studies can examine how the physical structure of the composite influences nonlinearity in terms of density, percent heaviness, LAC, and HVL. By manipulating the distance of the material from the radiation source or adding layers of the composite, investigations can be made on improving shielding performance. Moreover, tests on lifetime degradation may help evaluate the durability and lifetime use of the material. Lastly, future work can focus on assessing the economic feasibility of the composite and the environmental impact of its disposal.

Additional Information

Author Contributions

All authors have reviewed the final version to be published and agreed to be accountable for all aspects of the work.

Concept and design: Kyle Noah D. Esguerra, Jan Isiah S. Dela Cruz, John Dominic L. Sapao, Randy Joseph G. Fernandez

Acquisition, analysis, or interpretation of data: Kyle Noah D. Esguerra, Jan Isiah S. Dela Cruz, John Dominic L. Sapao, Randy Joseph G. Fernandez

Drafting of the manuscript: Kyle Noah D. Esguerra, Jan Isiah S. Dela Cruz, John Dominic L. Sapao, Randy Joseph G. Fernandez

Critical review of the manuscript for important intellectual content: Kyle Noah D. Esguerra, Jan Isiah S. Dela Cruz, John Dominic L. Sapao, Randy Joseph G. Fernandez

Supervision: Randy Joseph G. Fernandez

Disclosures

Human subjects: All authors have confirmed that this study did not involve human participants or tissue. **Animal subjects:** All authors have confirmed that this study did not involve animal subjects or tissue. **Conflicts of interest:** In compliance with the ICMJE uniform disclosure form, all authors declare the following: **Payment/services info:** All authors have declared that no financial support was received from any organization for the submitted work. **Financial relationships:** All authors have declared that they have no financial relationships at present or within the previous three years with any organizations that might have an interest in the submitted work. **Intellectual property info:** A Utility Model is planned for filing in the Philippines, for a product with a process for manufacture and use. As per Philippine law, copyright is granted from the moment of creation of the document. **Other relationships:** All authors have declared that there are no other relationships or activities that could appear to have influenced the submitted work.

Acknowledgements

Data are available on reasonable request to RJGF (rgfernandez@clc.pshs.edu.ph). All authors disclose support for the research in this work from the DOST-Philippine Science High School System. All authors disclose the use of the two-roll machine and compression molding machine for the research in this work from the DOST-Industrial Technology Development Institute. All authors disclose the use of the Cesium-137 radiation testing apparatus for the research in this work from the DOST-Philippine Nuclear Research Institute.

References

1. World Nuclear Association. Radioisotopes in Medicine. (2025). Accessed: January 10, 2025: https://world-nuclear.org/information-library/non-power-nuclear-applications/radioisotopes-research/radioisotopes-in-....
2. Foray N, Bourguignon M, Hamada N: Individual response to ionizing radiation. Mutation Research/Reviews in Mutation Research. 2016, 770:369-86. 10.1016/j.mrrev.2016.09.001
3. Ali YF, Cucinotta FA, Ning-Ang L, Zhou G: Cancer risk of low dose ionizing radiation. Frontiers in Physics. 2020, 8:10.3389/fphy.2020.00234
4. Cheon BK, Kim CL, Kim KR, et al.: Radiation safety: a focus on lead aprons and thyroid shields in interventional pain management. The Korean Journal of Pain. 2018, 31:244-52. 10.3344/kjp.2018.31.4.244
5. Santivasi WL, Xia F: Ionizing radiation-induced DNA damage, response, and repair. Antioxidants and Redox Signaling. 2014, 21:251-59. 10.1089/ars.2013.5668
6. Arif Sazali M, Rashid NKA, Hamzah K: A review on multilayer radiation shielding. IOP Conference Series Materials Science and Engineering. 2019, 555:012008. 10.1088/1757-899x/555/1/012008
7. More CV, Alsayed Z, Badawi MS, Thabet AA, Pawar PP: Polymeric composite materials for radiation shielding: a review. Environmental Chemistry Letters. 2021, 19:2057-90. 10.1007/s10311-021-01189-9
8. AbuAlRoos NJ, Baharul Amin NA, Zainon R: Conventional and new lead-free radiation shielding materials for radiation protection in nuclear medicine: A review. Radiation Physics and Chemistry. 2019, 165:108439. 10.1016/j.radphyschem.2019.108439
9. World Health Organization. (2022). Accessed: October 23, 2022 : https://www.who.int/news/item/23-10-2022-almost-1-million-people-die-every-year-due-to-lead-poisoning--with-more-chil....
10. Mourtada F, Clement CH, Dauer LT, et al.: Occupational radiological protection in brachytherapy. Annals of the ICRP. 2021, 50:5-75. 10.1177/01466453211013514
11. Bijanu A, Arya R, Agrawal V, et al.: Metal-polymer composites for radiation protection: a review. Journal of Polymer Research. 2021, 28:392. 10.1007/s10965-021-02751-3
12. Al-Buriahi MS, Eke C, Alomairy S, Yildirim A, Alsaeedy HI, Sriwunkum C: Radiation attenuation properties of some commercial polymers for advanced shielding applications at low energies. Polymers for Advanced Technologies. 2021, 32:2386-396. 10.1002/pat.5267
13. Soylu HM, Lambrecht FY, Ersöz OA: Gamma radiation shielding efficiency of a new lead-free composite material. Journal of Radioanalytical and Nuclear Chemistry. 2015, 305:529-34. 10.1007/s10967-015-4051-3
14. Chen S, Nambiar S, Li Z, et al.: Bismuth oxide-based nanocomposite for high-energy electron radiation shielding. Journal of Materials Science. 2018, 54:3023-34. 10.1007/s10853-018-3063-0
15. Sivasubramanian P, Chang JH, Nagendran S, Dong CD, Shkir M, Kumar M: A review on bismuth-based nanocomposites for energy and environmental applications. Chemosphere. 2022, 307:135652. 10.1016/j.chemosphere.2022.135652
16. El-Sharkawy RM, Abdou FS, Gizawy MA, Allam EA, Mahmoud ME: Bismuth oxide nanoparticles (Bi2O3 NPs) embedded into recycled- Poly(vinyl chloride) plastic sheets as a promising shielding material for gamma radiation. Radiation Physics and Chemistry. 2023, 208:110838. 10.1016/j.radphyschem.2023.110838

17. Akman F, Oğul H: Interaction parameters of some polymers used in nuclear power plants with ionizing radiation, produced secondary radiations and radiation damages. Macromolecular Materials and Engineering. 2024, 310:2400326. 10.1002/mame.202400326
18. Ashby MF: Materials Selection in Mechanical Design (4th ed). Elsevier, 2011.
19. Alsayed Z, Badawi M, Awad R, Thabet A, El-Khatib A: Study of some γ-ray attenuation parameters for new shielding materials composed of nano ZnO blended with high density polyethylene. Nuclear Technology and Radiation Protection. 2019, 34:342-52. 10.2298/ntrp190718033a
20. Philippine Nuclear Research Institute. (2024). Accessed: October 30, 2024: https://www.pnri.dost.gov.ph/index.php/downloads/software/epixs.
21. Şakar E, Özpolat ÖF, Alım B, Sayyed MI, Kurudirek M: Phy-X / PSD: Development of a user friendly online software for calculation of parameters relevant to radiation shielding and dosimetry. Radiation Physics and Chemistry. 2020, 166:108496. 10.1016/j.radphyschem.2019.108496
22. ASTM International: Standard Practice for Compression Molding Thermoplastic Materials into Test Specimens, Plaques, or Sheets (ASTM D4703-16). ASTM International, 2025. 10.1520/D4703-16
23. International Organization for Standardization: Rubber — Assessment of carbon black and carbon black/silica dispersion — Rapid comparative methods (ISO 11345:2006). International Organization for Standardization, 2006. https://www.iso.org/standard/40388.html.
24. Kausar A: Contemporary applications of carbon black-filled polymer composites: An overview of essential aspects. Journal of Plastic Film & Sheeting. 2017, 34:256-99. 10.1177/8756087917725773
25. Nurhajati DW, Lestari UR, Setyorini I, Mayasari HE: Effect of carbon black/Bi2O3 ratio on the vulcanization characteristic and mechanical properties of rubber compound. Macromolecular Symposia. 2020, 391:1900171. 10.1002/masy.201900171
26. Vicuña CV, Tumlos R, Salapare H, Fernandez RJ: Development of a New Lead-free Radiation Shield for Gamma Radiation using a WC-SBR Composite. 2017.
27. Kaundal RS: Comparative study of radiation shielding parameters for bismuth borate glasses. Materials Research. 2016, 19:776-80. 10.1590/1980-5373-mr-2016-0040
28. Madbouly AM, Sallam OI, Issa SAM, Rashad M, Hamdy A, Tekin HO, Zakaly HMH: Experimental and FLUKA evaluation on structure and optical properties and γ-radiation shielding capacity of bismuth borophosphate glasses. Progress in Nuclear Energy. 2022, 148:104219. 10.1016/j.pnucene.2022.104219
29. Muthamma MV, Bubbly SG, Gudennavar SB, Narendranath KCS: Poly(vinyl alcohol)-bismuth oxide composites for X-ray and γ-ray shielding applications. Journal of Applied Polymer Science. 2019, 136:47949. 10.1002/app.47949
30. Soheilmoghaddam M, Adelnia H, Bidsorkhi HC, Sharifzadeh G, Wahit MU, Akos NI, Yussuf AA: Development of ethylene-vinyl acetate composites reinforced with graphene platelets. Macromolecular Materials and Engineering. 2016, 302:1600260. 10.1002/mame.201600260
31. Astuti Y, Musthafa F, Arnelli A, Nurhasanah I: French fries-like bismuth oxide: physicochemical properties, electrical conductivity and photocatalytic activity. Bulletin of Chemical Reaction Engineering and Catalysis. 2021, 17:146-56. 10.9767/bcrec.17.1.12554.146-156
32. Kabir M, Unal F, Akinci TC, Martinez-Morales AA, Ekici S: Revealing GLCM metric variations across a plant disease dataset: a comprehensive examination and future prospects for enhanced deep learning applications. Electronics. 2024, 13:2299. 10.3390/electronics13122299
33. Kobayashi T, Sundaram D, Nakata K, Tsurui H: Gray-level co-occurrence matrix analysis of several cell types in mouse brain using resolution-enhanced photothermal microscopy. Journal of Biomedical Optics. 2017, 22:036011. 10.1117/1.jbo.22.3.036011
34. O'Byrne M, Ghosh B, Pakrashi V, Schoefs F: Texture Analysis based Detection and Classification of Surface Features on Ageing Infrastructure Elements. BCRI2012 Bridge & Concrete Research in Ireland. 2012,
35. Intom S, Kalkornsurapranee E, Johns J, et al.: Mechanical and radiation shielding properties of flexible material based on natural rubber/ Bi2O3 composites. Radiation Physics and Chemistry. 2020, 172:108772. 10.1016/j.radphyschem.2020.108772
36. Li W, Peng M, Zhao X, Chen S: Properties of Bi2O3/epoxy resin-coated composites for protection against gamma rays. Journal of Industrial Textiles. 2022, 51:7545S-568S. 10.1177/15280837211051102
37. Singh VP, Badiger NM, Chanthima N, Kaewkhao J: Evaluation of gamma-ray exposure buildup factors and neutron shielding for bismuth borosilicate glasses. Radiation Physics and Chemistry. 2014, 98:14-21. 10.1016/j.radphyschem.2013.12.029
38. Halimah MK, Azuraida A, Ishak MR, Hasnimulyati L: Influence of bismuth oxide on gamma radiation shielding properties of boro-tellurite glass. Journal of Non-Crystalline Solids. 2019, 512:140-47. 10.1016/j.jnoncrysol.2019.03.004
39. Tochaikul G, Tanadchangsaeng N, Panaksri A, Moonkum N: Enhancing radiation shielding capabilities with epoxy-resin composites reinforced with coral-derived calcium carbonate fillers. Polymers. 2025, 17:113. 10.3390/polym17010113